Tailoring Metal–Organic Frameworks for CO2 Capture: The Amino Effect

ARTICLE *in* CHEMSUSCHEM · SEPTEMBER 2011

Impact Factor: 7.66 · DOI: 10.1002/cssc.201000458 · Source: PubMed

4 AUTHORS, INCLUDING:

Jenny G Vitillo
Università degli Studi dell'Insubria
72 PUBLICATIONS **1,866** CITATIONS
SEE PROFILE

Gabriele Ricchiardi
Università degli Studi di Torino
89 PUBLICATIONS **4,213** CITATIONS
SEE PROFILE

DOI: 10.1002/cssc.200((will be filled in by the editorial staff))

Tailoring MOFs for CO_2 capture: the amino-effect

Jenny G. Vitillo,*[a] Marie Savonnet,[b] Gabriele Ricchiardi[a] and Silvia Bordiga[a]

((Dedication, optional))

Carbon dioxide capture from process is one of the strategies adopted to decrease anthropogenic greenhouse gases emissions. In order to lower the cost associated with the regeneration of amine-based scrubbers systems, one of the envisaged strategies is the grafting of amines on high surface area supports and in particular on metal-organic frameworks (MOFs). In this study, the interaction between CO_2 and aliphatic and aromatic amines has been characterized by quantum mechanical methods (MP2), focusing the attention both on species already reported in MOFs and on new amine-based linkers, in order to inspire the rational synthesis of new high-capacity MOFs . Calculations highlights binding site requisites, and indicate that CO_2 vibrations are quite independent on the adsorption energy and their monitoring in probe-molecule experiments is not a suitable marker of efficient adsorption.

Introduction

The increase in greenhouse gases concentration in the terrestrial atmosphere is one of the grand problems of the present century. It is in fact nowadays clear that a strict relationship exists between carbon dioxide atmospheric concentration and air-temperature.[1] In particular, from the analysis of the Vostok and Dome C stations data, it is evident that any change in the CO_2 and CH_4 concentration is always followed, with a certain delay, by a proportional change in the air-temperature. The sheer increase in the atmospheric carbon dioxide concentration, evidenced by the data recorded at the Mauna Loa observatory,[2] has then caused alarm not only because of their trend but even more for the recorded absolute CO_2 concentration values: in 2009 the CO_2 concentration amounted to about 390 ppm, that is one third larger than the highest value measured over the past 740,000 years, a period interested by both ice ages and warm periods. The duty to find a solution to invert this trend and mitigate its consequences is then mandatory. However, if on one hand it is important to reduce greenhouse gas emissions by increasing the energy efficiency of the existing technologies and by adopting less-CO_2 emitting energy sources, a more practical and direct approach to solve the problem is CO_2 capture. Moreover, CO_2 capture deserves the greatest attention also as the first step in CO_2 conversion to chemicals and fuels (see for instance synthetic photosynthesis). In this context, two strategies can be adopted: (i) capturing the atmospheric CO_2 (DAC, direct air capture), in order to reduce the concentration of the CO_2 already present in the atmosphere;[3] (ii) capturing the CO_2 present in the flue gases, to avoid any increase in its concentration by reducing the CO_2 anthropogenic emissions. In particular, as far as the second approach is concerned, the main stream of the research is concentrated in the design of processes for CO_2 capture in power plants based on the combustion of fossil fuels, that account for 86% of the total anthropogenic greenhouse gas emissions.[4, 5] The capture process can be placed before or after the fuel combustion: in the former case it is a mere separation problem, while in the latter it consists in a previous more or less complex fuel processing step leading to CO_2 and a carbon-free fuel (typically hydrogen). Therefore, the separation step is characterized by sensitively different working pressures and temperatures. In fact, whereas in a post-combustion process the temperature is only slightly different from RT and the pressure is around 1 bar, for the pre-combustion purification the temperature can be as high as 400 °C with pressures sensitively larger than the atmospheric one.[6] The materials needed as CO_2 scrubbers are then sensitively different for the two technologies. Another important difference between the pre- and the post-combustion processes are the gases involved in: post-combustion capture, in fact, can be approximately seen as a CO_2/N_2 separation, being essentially an air purification from CO_2, whereas in pre-combustion technologies $H_2/CO/CO_2$ separations are crucial.[4]

Although promising, the pre-combustion methods are expected to have only limited application in the short and middle term, being the pre-existing available technology fundamentally of post-combustion type. The improvement of the performances of the post-combustion technology would be the most beneficial and more applicable solution to the greenhouse gas problem in short

[a] *Dr. J. G. Vitillo, Dr. G. Ricchiardi, Prof. S. Bordiga*
Dipartimento di Chimica IFM and NIS Centre of Excellence,
Università di Torino, INSTM UdR Università
Via Pietro Giuria 7, 10125 Torino, Italia
Fax: (+39) 0116707855
E-mail: jenny.vitillo@unito.it

[b] *Dr. M. Savonnet*
IFP Energies Nouvelles
BP n°3, 69360, Solaize, France
IRCELYON, University of Lyon 1
CNRS, 2 avenue Albert Einstein, F-69626, Villeurbanne Cedex

Supporting information for this article is available on the WWW under http://www.chemsuschem.org or from the author.

term. In particular, between the envisaged CO_2 capture technologies, the amine–based scrubbing is the most mature and used in post-combustion air purification processes. Nevertheless, although it has been employed on an industrial scale for over 50 years because of its high separation efficiency and its ability to work in a wet environment, the amines technology suffers a number of drawbacks.[4, 7] Beside the amines are flammable, corrosive and toxic,[8] they are also sensitive to oxidation with release of toxic products and their regeneration is energy intensive. In particular, it has been estimated that the regeneration energy would accounts for 25-40% of the power generated in the plant, a cost that is hardly sustainable. On the other hand the thermodynamic minimum energy loss is one order of magnitude smaller, a fact that prompts for active research of alternative scrubbers..[4] The reasons of such a large current energy cost are associated to the great stability of the carbamate and carboxylate species formed upon the reaction with CO_2 but also to the presence of a great amount of water (the solvent). Actually, the presence of water, because of its high thermal capacity, requires the waste of a large amount of heat to bring the amine solution to the regeneration temperatures (80-140°C). Fifty years of research have allowed to identify different ways to improve the performances of the amine technology, by lowering the stability of the reacted species or avoiding the presence of the solvent.[9] For what concerns the latter, a stratagem is to disperse the amines on high surface area solid supports and many studies employing almost all classes of materials have been already reported, e.g. zeolites,[10] mesoporous siliceous materials,[7, 9, 11] xerogels,[12] polymers[13] and MOFs.[14-22] High cyclability, high CO_2 uptake and thermal stability in the range for the regeneration of the system (25-140°C) are the necessary requirements for the industrial use of an amino-supported material as CO_2 scrubber. They can be assured by three main features:[7] (i) the presence of a covalent bond between the group bearing the amine functionalities and the support; (ii) high amine loadings (>6 mmol N/g);[23] (iii) moisture resistance. Among the different classes of supports, MOFs are receiving a great interest[18, 19, 24, 25] because of the flexibility in their synthesis that allows not only to tune the pore size and topology in a wide range, but also because of the chemical composition of the framework, allowing to tune at the molecular level the affinity of the material toward CO_2 by means of: metal substitution, ligand substitution and ligand functionalization. It is then not surprising that the CO_2 capacities of MOFs are among the largest reported so far[26, 27] and that they have shown promising performances also in separation processes, as CO_2/N_2 (postcombustion),[26, 28, 29] CO_2/H_2 (precombustion),[28] CO_2/CO (steel industry)[30] and CO_2/CH_4 (natural gas sweetening)[18, 26, 28, 31] separations.

It has been claimed that the presence of nitrogen atoms[32, 33] and in particular the functionalization by amino groups[14, 19, 22, 24, 25, 34] is a valuable way to increase the MOFs affinity toward CO_2, with benefits on the adsorbed quantities and on the separation selectivities. Nevertheless, little attention is in general paid on the different amines types present in the framework and on their different affinity and ability to bind CO_2. Both aromatic and aliphatic amines have been dispersed in MOFs. For what concerns aromatic amines,[14, 19-22, 25] they are in general introduced in the framework during synthesis, by using linkers bearing a $–NH_2$ functionality. Aliphatic amines, on the contrary, are introduced in the MOF frameworks with post-synthesis reactions involving (i) the open metal centers[16, 17] or (ii) a pre-existing aromatic $–NH_2$ groups.[35, 36] In the first case the amine is coordinated by the metal center, whereas in the second case the aromatic amino-group is converted in a functional group bearing an aliphatic amine by using aziridine reactions[35] or the click-chemistry,[36] with the advantage over (i) that a chemical bond between the MOF and the amine is formed, assuring the stability of the grafted species.

Among the experimental techniques for the molecular understanding of CO_2 binding and reactivity towards amines, besides the obvious gravimetric, volumetric and calorimetric studies, probe-molecule experiments using infrared spectroscopy have been extensively used, following a general trend in studies of adsorption and catalysis, where this technique is highly informative on site-specific molecular interactions.[19, 33, 34, 37-40]

During the past years, quantum mechanical studies on the interaction between CO_2 and amines were mainly targeted to the study of supercritical CO_2 as an alternative to toxic organic solvents in industrial applications,[41, 42] and in particular as dispersion medium in the synthesis of polymeric materials as polyurethane.[42, 43] Studies have been also performed on the interaction between CO_2 and polymers.[13, 41] Only recently, some works concerning the interaction between CO_2 and MOFs have appeared.[19, 33, 34, 37-40] In particular, Vogiatzis et al.[33] have reported a very detailed study on the CO_2 interaction with N-containing organic heterocycles to be used as MOF linkers. On the other hand, a computational evaluation of probe-molecule experiments, i.e. an accurate description of NH_2 perturbed CO_2 vibrations is still lacking. In this work, the possibility to tune the MOFs affinity for CO_2 has been studied by means of quantum chemical simulations at the MP2 level by considering CO_2 interactions with the cluster models reported in Scheme 1. The possibility to correlate the binding energies with the changes in CO_2 geometry and vibrations has been also investigated. In a first step, the interaction with benzene-1,4-dicarboxylic acid has been considered because it represents the basic linker in most MOFs;[17, 19, 22, 25] two cluster models have been adopted: benzene (**1**) and benzene-1,4-dicarboxylic acid (**1'**). Three different types of amino-functionalities have been then considered: (i) aromatic amines,[14, 19-22, 25] (ii) aliphatic amines as part of the substituent group on the ring,[35, 36] (iii) aliphatic amines grafted on an open metal center.[16, 17] For what concerns the aromatic amines, aniline (**2**), 2-amino-1,4-benzenedicarboxylic acid (**2'**), 1,2-amino-benzene (**3**), and adenine (**14**) have been used. The **3** model has been adopted also in order to study the contemporary interaction of CO_2 with two $-NH_2$ groups: in fact, the random distribution of the $-NH_2$ substituents in the MOF frameworks makes it likely the presence of $-NH_2$ pairs in the material (although belonging to two different rings). Aliphatic amines introduced by aziridation have been modeled with N-phenyl-1,2-ethanediamine (**4**). 4-methylamino-1,2,3-triazole (**5**), 4-methylamino-1,2,3-triazol-1-phenyl (**5'**), 4-dimethylaminomethylene-1,2,3-triazole-1-phenyl (**6**), 4-diethylaminomethylene-1,2,3-triazole-1-phenyl (**7**) have been adopted as models for possible aliphatic amines grafted by means of click-on reactions. These models have been adopted in order to study the adsorption on primary and tertiary amines and the dependence of the CO_2 affinity on the dimension of the N-substituents. Ethylenediamine grafted on 3-Zn-di-1,2,3-triazole (**10**) has been used as model for ethylenediamine in interaction with open metals in MOFs. For comparison, the two adducts have been also simulated separately (**8** and **9**), in order to quantify the benefit of the introduction of the amine (if any) in the MOF. Other functionalities as $-N_3$ (azidebenzene, **11**), $-NO_2$ (nitrobenzene, **12**),[18, 22] and -Br (bromobenzene, **13**)[18, 22] have been considered and their energetics compared to the amines ones. In the end, the interaction of CO_2 with Al-OH (**16**),[14, 29] Ga-OH (**17**),[44] and In-OH (**18**)[44] hydroxyls, often present as competitive adsorption sites in MOFs have been studied. The interaction with silanol (**15**)

has been also taken into account as rough model of the most energetic species in silicalite, because of the experimental use of the CO_2 modes in silicalite as reference for the CO_2 shift.[45]

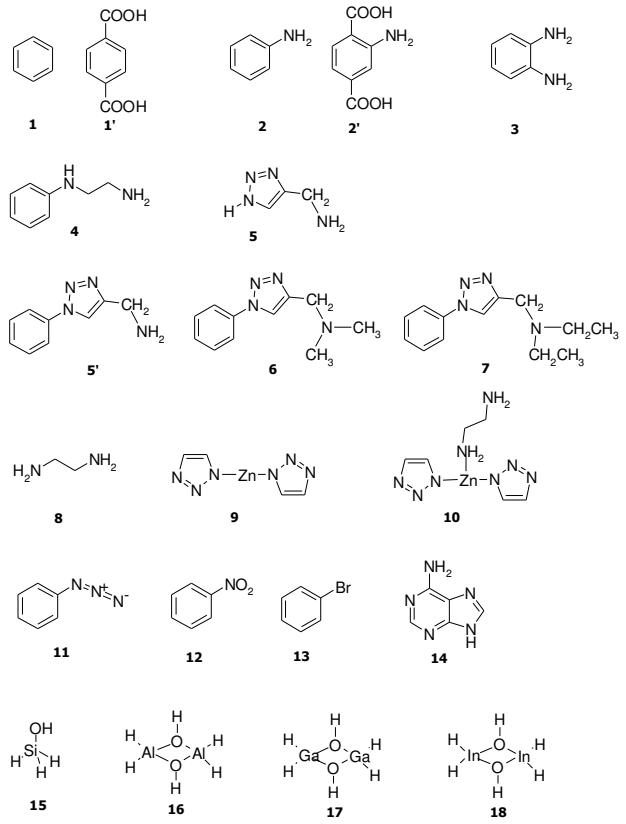

Scheme 1.

Results and Discussion

The CO_2 molecule response to ESPs

Carbon dioxide is a linear molecule with $D_{\infty h}$ symmetry (calculated $d_{C\text{-}O}$ = 1.170 Å at MP2/TZV2p, close to the experimental value of 1.163 Å). The large charge separation in the C=O bonds (q_C = -2q_O = 0.735449 *e*, Mulliken analysis, MP2/TZV2p) is responsible of the significant quadrupole moment of the molecule.[46] The quadrupolar shape of the CO_2 electrostatic potential (ESP) with a positive doughnut in the C plane and two negative lobes on the molecular axis is evident in the map reported in Figure 1. In particular, if the molecule is aligned along the *z* axis, the components of the electrostatic quadrupole are $\Theta_{xx} = \Theta_{yy} = -1/2\Theta_{zz} = 1.3924$ Debye · Å (MP2/TZV2p, traceless tensor, referred to the molecular center of mass coincident with the coordinate origin and in the Buckingham notation). Because of its quadrupolar nature, CO_2 can act both as a Lewis acid and a Lewis base:[46] on purely electrostatic basis CO_2 interacts with negative charges in a side-on geometry through a direct interaction with the C,[47] whereas in the case of positive charges end-on adducts through one oxygen are formed.[45] However, experiments and calculationst[34, 48] converge in indicating that adsorption is a complex interplay of dispersion forces and electrostatics, favoring cooperative adsorption based on the interaction through both the C and O atom with the material and CO_2-CO_2 interactions.

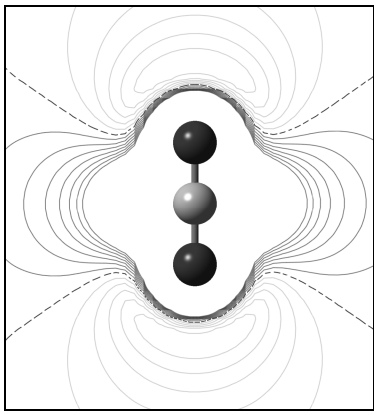

Figure 1. Electrostatic potential map of CO_2 molecule in the plane of the atoms, as obtained at the MP2/TZV2p level. Solid black, dashed black and solid grey lines correspond to positive, zero and negative potentials respectively, in the range between -0.028 a.u. and +0.028 a.u., separated by 0.004 a.u.. Dimensions of the rectangle: 7.5×6.8 Å.

Carbon dioxide is characterized by three vibrational modes: the IR-inactive symmetric stretching mode $\tilde{\nu}_1$, the doubly degenerated bending vibration $\tilde{\nu}_2$ and the asymmetric stretching mode $\tilde{\nu}_3$. Upon interaction with the materials these modes are only slightly shifted, even when highly charged species are present.[45] The shift of the CO_2 vibrations upon adsorption give some insight into the adsorption geometry and the nature of the adsorption site. Nevertheless, the presence of a negative charge, although leaving identical (and elongated) the two C=O bonds, causes a change in the ∠OCO angle: this corresponds to the decrease of the $\tilde{\nu}_3$ mode and to the removal of the degeneracy for the $\tilde{\nu}_2$ mode. This results spectroscopically into an increase of the asymmetric stretching mode frequency. On the contrary, in the case of adsorption on a positive charge the molecule is still linear but the two C=O bond are no more identical: the C-O bond adjacent to the cation lenghtens slightly whereas the other C-O bond shortens of almost the same amount.

Structure and stability of carbon dioxide complexes

The coordinates obtained from the optimization of the isolated clusters and of the corresponding CO_2 adducts are reported in the Supporting Information. Different minima can be found for the adsorption of CO_2 on the clusters reported in Scheme 1. In particular, more than one geometry of interaction was considered for the **2**, **4**, **5**, **5'**, **12**, **13** and **14** clusters (see also Figure S2). The structures of the adducts that will constitute the main topic of the following discussion are reported in Figure 2 and their main geometrical and energetic parameters are reported in Table 1. In Table S1 and S2, a more exhaustive summary of the results obtained for all the adducts is presented.

Table 1. Average deformation of the CO_2 bond angle [°] in the CO_2 adducts with the molecules reported in Scheme 1, distances between the clusters and the carbon of CO_2 and between the clusters and one of the CO_2 oxygens [Å], and BSSE-corrected binding energies [kJ mol-1] calculated at the MP2/TZV2p level of theory. The C=O bonds are unaffected by the interaction (changes < 0.001 Å).

system	$\Delta\angle$OCO[a]	r(C-X)[b]	r(O-X)[b]	BE[c]
1	1.0	3.290	3.416	9.1
1'	0.4	3.215	3.250	9.9
2a	1.4	2.982	3.323	13.7
2'	0.8	3.135	3.144	8.8
3	1.7	2.967	2.592	16.2
4a	2.6	2.930	2.910	11.3
5a	2.4	2.952	2.572	13.0
5'a	2.8	2.959	3.039	14.3
6	4.1	2.807	2.514	17.1
7	3.8	2.908	2.644	15.4
8	3.1	2.896	3.300	11.5
9	6.0	2.669	2.220	28.2
10	2.8	2.939	2.625	12.3
11	0.4	3.144	3.107	10.7
12a	0.5	3.137	3.095	9.5
13a	0.7	3.197	3.147	9.5
14a	3.1	2.852	2.341	12.6
15	1.9	2.802	3.039	9.5
16	1.0	3.769	2.175	11.2
17	0.6	3.641	2.250	9.4
18	1.0	3.868	2.296	8.8

[a] Calculated values for unperturbed CO_2 at the MP2/TZV2p: $\angle$OCO = 180°C. [b] r(C-X) (and r(O-X)) represents the shortest distance between the carbon atom (one of the oxygens) of CO_2 and one atom of the cluster. For the clusters containing a $-NH_2$ directly interacting with CO_2, r(C-X) coincides with the distance from the N atom of the amino group.

It is evident in Figure 2 that in all the adducts the interaction between CO_2 and the clusters is obtained through both the carbon and at least one of the oxygens. This was expected because of the Lewis acid-base nature of CO_2. Moreover, this agrees with previous calculations[33, 37, 38, 42] and with the geometry of interaction expected on the basis of the electrostatic potential (ESP) maps of the isolated clusters (reported in Figure S1 in the Supporting information): side-on for the **1-15** adducts and end-on for the **9** and **16-18** ones. The usefulness of the ESP maps in predicting the different stability of CO_2 adducts has been reported in a previous study concerning the interaction between CO_2 and N-containing heterocycles.[33] Also in the adduct **9** where a strong positive Zn^{2+} center is present, a side-on geometry was obtained because of the high negative potential on the N=N pair of the triazolate ring in **9**, responsible of the low $r_{C\text{-}X}$ value. For what concerns the **16**, **17** and **18** complexes (hydroxyls) an end-on configuration was found for CO_2 with respect to the H atom of the hydroxyl group. This geometry is different with respect to the one evidenced for the interaction with Si-OH in the **15** adduct, where CO_2 is side on with respect to the hydroxyl. This dissimilarity can be ascribed to the different negative-positive ESP balance in the O-H couple in these four hydroxyl species. The strength of the interaction decreases in the order Al > Si~Ga > In, accordingly to the $r_{O\text{-}H}$ (Al < Ga < In, see Table 1). Being possible in some cases (e.g. MIL-53) to synthesize isostructural Al-, Ga- and In-based MOFs with hydroxyl species, these calculations indicate as an higher affinity toward CO_2 is expected for the Al-MOFs.

As far as the interaction with arenes is concerned (**1**, **1'**, **2a**, **2'**, **3**, **11**, **12a**, **13**, **14a**), CO_2 is oriented parallel to the ring in all the adducts because of the π–quadrupole interaction. However, in none of them it is placed on the center of the ring: when a polar group is present on the ring as substituent, the global minimum is always the result of a direct interaction of CO_2 with the group.[37, 38] This holds also in the case of benzene (**1**) where CO_2 is slightly displaced from the center of mass of C_6H_6, in order to allow the oxygen to interact with one of the positively charged H. This is in disagreement with previous calculations conducted at a lower level of approximation (PW91/DNP)[37, 38] that indicated a more symmetric geometry for the CO_2/C_6H_6 system. For what concerns aniline, the BE[c] obtained is close to that reported in refs. [38, 42] (14.3 at MP2/aug-cc-pVDZ and 11.9 kJ mol^{-1} at MP2/6-311+G(2d,2p)//PW91/DNP) but lower than that reported in ref. [19] (20 kJ mol^{-1}), that however was not corrected for the BSSE, which is not negligible in interactions where the dispersion component is prevailing (compare the corrected and uncorrected BE values reported in Table S1 in the Supporting Information).

It is important to notice that BE[c] was always larger than that obtained for benzene for both electron-acceptor (-COOH, **1'**, $-N_3$, **11**, $-NO_2$, **12**, and -Br, **13**) and electron-donor ($-NH_2$, **2**, **3**) substituents. This was a further proof that the interaction does not involve only the π orbitals of the arene, because in this case a decrease in the BE[c] would be observed for electron-acceptor substituents. There is only one exception, represent by **2'** that however is ascribable to the larger deformation energy (DE) obtained for this adduct (3.4 vs. 0.1 kJ mol^{-1}): if the DE energy is considered, the interaction energy becomes 12.2 kJ mol^{-1} that is larger than that obtained for **1** and **1'** but lower than that obtained for **2** (**2** > **2'** > **1'** > **1**). In fact in **2'** the ESP on the N atom of the $-NH_2$ group is less negative than in **2** because of the presence of the electron acceptor –COOH group on the ring. The same effect is observed if N is present as heteroatom in the ring as in adenine (**14**). In this case the BE[c] for the CO_2/NH_2 interaction would be of only 11.6 kJ mol^{-1} (**14a** adduct, see Table 1). It is important to stress that **2'** is the actual linker present in most amino-MOFs that have been claimed in literature to possess an higher affinity for CO_2 with respect to the unfunctionalised ones. This higher affinity has been verified in literature for MIL-53(Al) by means of calorimetric (30 vs. 50[19] kJ mol-1 for the MIL-53(Al) and amino-MIL-53(Al) at the lower coverage), and chromatographic measurements (20.1 vs. 38.4[14] kJ mol^{-1}) and it has been associated to a direct interaction between the $-NH_2$ and the CO_2 molecule. This would be supported by the present calculations if **1** and **2** were used as models for the adsorption site. However, if the larger and more realistic clusters **1'** and **2'** are considered, the BE of the amino substituted complex is lower than that for the unsubstituted one.

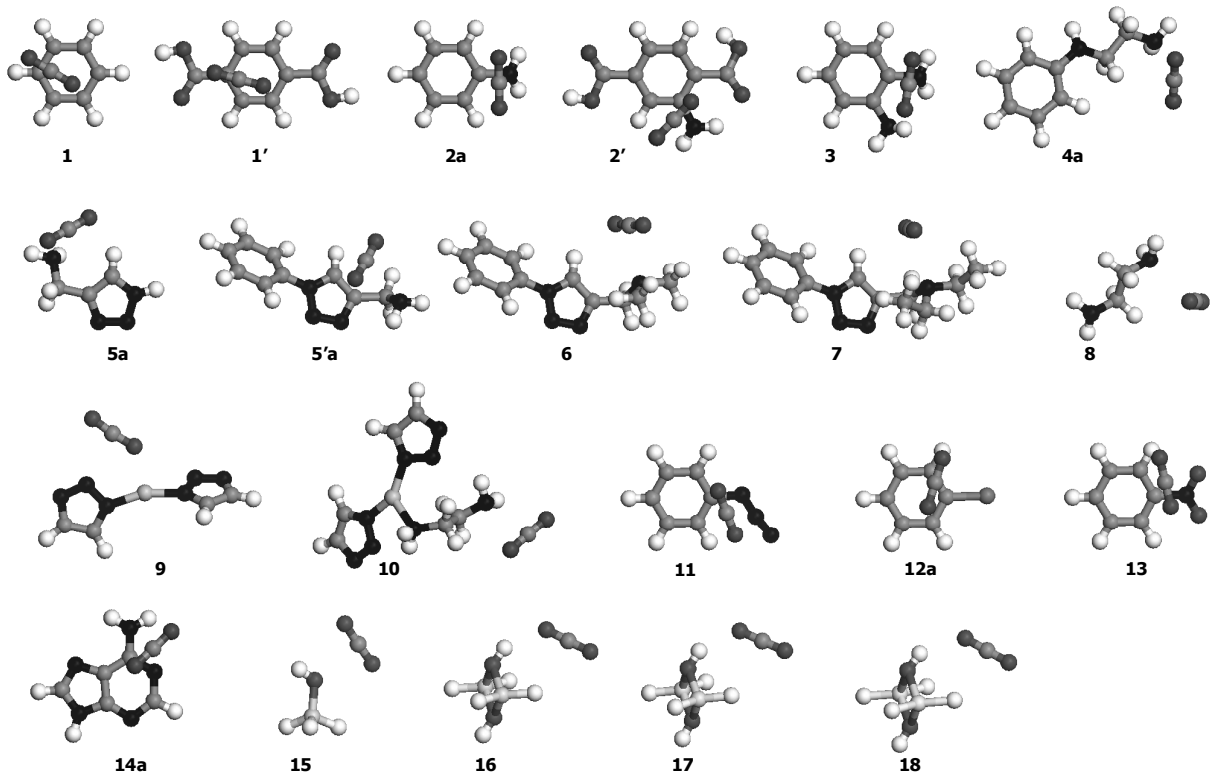

Figure 2. Geometries as obtained by optimization at the MP2/TZV2p level for the CO_2 adducts with the systems reported in Scheme 1. The atoms are represented as spheres with the gray code: N (black) > O > C > Br > Zn > Si > Al > Ga > In > H (white).

The **2'** model would indicate that the presence of the aromatic amines would be detrimental for CO_2 adsorption in terephtalate-based materials. Therefore, our calculations suggest that the experimentally observed higher affinity of NH_2-MOFs for CO_2 is not due to a site specific stronger interaction with the amino-group but rather to more complex interactions, e.g. interaction with multiple sites and the effect of the overall polarity of the structure. This has been verified in a very recent paper[34] where a periodic model has been adopted to study the CO_2 adsorption in MIL-53(Al) materials. The clusters here studied are a first approximation of the actual linker in the MOF. In fact, first of all, in a metal-organic framework, additional effects, both electronic and steric will come into play, and full periodic calculations on model materials will be necessary to investigate for instance, how steric hindrance might affect the accessibility of the adsorption sites and their interaction with CO_2.[37] This is even more important in "breathing" materials such as MIL-53. An estimate of the energetic contribution coming from the pore can be evaluated in a first approximation by comparing the GCMC calculated adsorption enthalpies of CO_2 in the "narrow pores" and the "large pores" configuration of MIL-53(Al)[49] that amounts to 37 and 17 kJ mol^{-1}, respectively). Their difference would account for almost the whole difference between the BE^c obtained for the present model (9.9 kJ mol^{-1}) and the experimental value (30 kJ mol^{-1}) for MIL-53(Al).

Concerning the interaction with multiple sites, it is interesting to note that when two aromatic $–NH_2$ functionalities are present on the ring (**3**), the BE is increased by about the 20%. This is due on one hand to the increase of the ESP values on the ring, because of the well known additive effect on the ESP with respect to the number of substituents on the ring.[37, 50] On the other hand, the presence of a -NH_2 pair allows the simultaneous interaction of CO_2 through C with the N atom of one $–NH_2$ and through one O with the H atoms of the second $–NH_2$. These two interactions have similar BEs (see **2b** cluster Supporting Information and Ref. [38]). This means that if two $–NH_2$ pair is present, the adsorption enthalpy could be significantly increased with respect to a single $–NH_2$ and then to an unfunctionalised MOF. The presence of this pair is possible because of the random distribution of the amino-functionalities in the MOFs. A rough estimation of the probability to have neighboring $–NH_2$ pairs in MIL-53(Al)-NH_2 by using a simple stochastic model has allowed to guess that the 33% of the $–NH_2$ group in this material are involved in a pair (see Supporting Information for details). Their presence would allow to explain the complex dependence of the isosteric heat q_{iso} on the CO_2 coverage observed experimentally for MIL-53(Al)-NH_2.[19] In fact, for MIL-53(Al) q_{iso} resulted to be completely independent on the coverage being its value fixed at 30 kJ mol^{-1} in the 0-1 bar pressure range. On the contrary, in MIL-53(Al)-NH_2 q_{iso} decreases from an initial 50 kJ mol^{-1} at zero coverage to values lower than those observed for the unsubstituted material at coverages as low as 0.15 (expressed as CO_2/NH_2 molar ratio) that is in conditions far from the saturation of the $–NH_2$ group by CO_2. If the effect of the presence of the amino would be simply the substitution of the **1'** linker with the **2'**, the expected effect would be a shift of the q_{iso} horizontal line to higher/lower values. On the basis of the present calculations the larger q_{iso} observed for $CO_2/NH_2 < 0.15$ would be ascribable to the interaction with the -NH_2 pairs, whereas for larger coverage the interaction with single $–NH_2$ functionalities would cause lower q_{iso} than that obtained in the unfunctionalised material. *Summarizing, we propose that the larger CO_2 affinity observed experimentally for 2-amino-1,4-benzenedicarboxylate-based materials is caused by the presence of pairs of $–NH_2$*

groups and not by the direct interaction with isolated –NH_2 groups.

As far as the interaction with aliphatic amines (**4**-**8**, **10**) is concerned, the BE significantly varies with the system considered. If the aliphatic amine is grafted directly to the ring as in **4** the BE^c for CO_2 interaction with -NH_2 is surprisingly lower (11.3 kJ mol^{-1}) than that obtained for the corresponding aromatic amine in spite of the higher basicity of aliphatic amines[42] (see **2**). However, the BE and the geometrical parameters in **4** are identical to those obtained for isolated ethylenediamine (**8**, EDA): the EDA chemical reactivity toward CO_2 is expected to be maintained unaltered after the grafting in the MOF, that could then act as a capture matrix avoiding the use of solvents. On the contrary, grafting an EDA molecule on an open metal center would cause a strong increase in the polarity and then on the reactivity of the amine (compare the ESP for **8** and **10** in Figure S2). The CO_2 BE^c is significantly lower on EDA in **10** than that calculated for CO_2 adsorption on the bare cation (**9**, 28.2 kJ mol^{-1}). This is in apparent disagreement with what observed experimentally: in ref. [16] a q_{iso} of 21 kJ mol^{-1} has been obtained for CO_2 adsorption on Cu-BTTri (a material with open Cu^{2+} centers) that results to be increased to 90 kJ mol^{-1}[16] after the grafting of ethylenediamine. Such a large difference between the calculated and experimental values is well beyond the accuracy of both calculations and measurements and therefore it can be taken as an indication of a chemical reaction of CO_2 with ethylenediamine, possibility not taken into account in the model. EDA coordinated to open metal sites in MOFs are expected to be greatly stable both thermally (BE^c_{EDA} = 152.8 kJ mol^{-1} in **10**) and in presence of water (BE^c_{H2O} = 108.6 kJ mol^{-1}), features that are interesting for a real use of these systems for CO_2 capture.

An alternative way to introduce aliphatic amines in MOFs is by using a click-on reaction. Following the procedure reported in ref. [36], the amine species would be linked to the organic spacer of the MOF through a triazolate. Three possible species have been here considered: a primary amine (-CH_2-NH_2 in **5**, **5'**) and two tertiary amines with a different dimension of the substituents on the N atom (–CH_2-$N(CH_3)_2$ in **6** and –CH_2-$N(CH_2CH_3)_2$ in **7**) in order to verify the effect of the dimension of the substituents on the BE. In these **5**-**7** clusters, two competitive adsorption sites are predicted on the basis of the ESP maps: the –NH_2 group of the aliphatic amine and the N=N pair on the triazolate ring. Among these two sites, the N=N resulted to possess a lower affinity for CO_2 in all the clusters but for **5**. However, in this case the largest stability of the N=N adduct was largely due to the involvement in the interaction of the H^+ proton of the N-H group (cluster **5b** in Figure S2) that is no more present in the larger cluster **5'**. The –NH^+ group is also responsible of the large BE^c (22.1 kJ mol^{-1}, MP2/TZVPP) obtained in ref. [33] for imidazopyridamine. This hydrogen is in fact characterized by a sensitively higher positive potential with respect of the H atom in benzene.

The dimension of the groups linked to the N atom of the amine has not a monotone influence on the ESP (and then on the BE^c). In fact, whereas an increase in the ESP values is obtained by substituting the primary amine –CH_2-NH_2 of **5'** with the tertiary amine –CH_2-$N(CH_3)_2$ of **6**, no further benefit is obtained by considering bulkier substituent as verified for –CH_2-$N(CH_2CH_3)_2$ (**7**). The reactivity of the amino functionalities are then in the order: **6** (CH_3) > **5'** (H) > **7** (CH_2CH_3). This trend is opposite with respect to what observed for calculations on aliphatic amines where the BE^c increases with the dimension of the substituents on the N atom going from ETA to TBA.[42] For what concerns the BE^c, it is worth noticing that an increase in the BE^c is observed from **5** to **5'**. This behavior is opposite to what observed for the other functionalities, where the introduction in MOFs (that is increasing the cluster size) causes a decrease in the CO_2 affinity of the group.

In Figure 3, the BE^c is reported as function of $r_{O\text{-}X}$ for **9**, **16**, **17** and **18** that is for the clusters were a predominance of the oxygen contribution can be evidenced and of $r_{C\text{-}X}$ for all the other systems. Also the data related to the **4b** and **14b** adducts characterized by a strong interaction between one of the CO_2 oxygen and the proton of the –NH group of the support are reported in the Figure 3. As a general statement, it is evident from this picture that when the interaction between CO_2 and the support is driven by one of the oxygen the distance of coordination is significantly lower that in the case of carbon (and then the density of CO_2 that can be achieved in the material would be higher). The larger distances observed in the latter case are ascribable to the large electronic repulsion due to the presence of the oxygen atoms on the both side of carbon that prevents small distances of coordination.

This picture gives also another important information: when the dispersion forces constitute the main contribution to the BE^c, the binding energies do not exceed 15 kJ/mol also if other functionalities than amines are considered. For what concerns the aliphatic amines, the BE^c are on average larger than those calculated for the aromatic amines, as expected due to the well-known higher basicity of the former. However, in order to avoid the chemical reaction between the material and CO_2 (that is, low regeneration energy) an aromatic amine would be preferable.

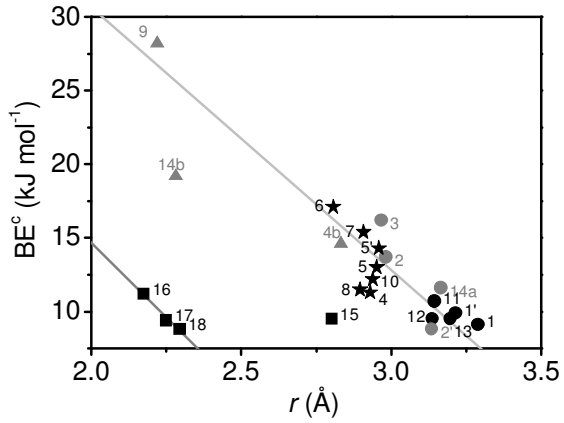

Figure 3. BE^c dependence on the CO_2 – cluster distance for CO_2 adducts. The different scatters refer to the different subsets: arenes (black circles), aromatic (gray circles), aliphatic amines (stars), hydroxyls (squares) and cationic species (triangles).

From the plot reported in Figure 3, it is evident as BE^c does not have a general dependence on the cluster-CO_2 distance (R^2 = 0.18 for a linear fit). Nevertheless, if the adducts are separated in two sets, a linear behavior can be evidenced, the first of this set constituted by almost all the clusters (**1-7**, **9-13**, **14a**, y = -17.83 *x* + 68.31, with R^2 = 0.87), whereas the second one is formed by the adducts with the Al-, Ga- and In-OH species (*y* = -20.24 *x* + 55.14 , with R^2 = 0.97). For what concerns the BE^c dependence on the deformation of the CO_2 molecule (both bond lengths and angle) an even more spread plot was obtained (not reported for the sake of brevity). As a general trend, a larger deformation of CO_2 corresponds to a larger affinity of the system towards CO_2 but a simple relationship between these quantities can not be evidenced.

Vibrational modes

On the basis of the calculated BEs, it would be difficult to predict what would be the preferential adsorption site in materials where more than one functionalities is present at the same time. For example, hydroxyl groups and organic linkers are both present in the structure of many MOFs as MIL-68 and MIL-53 and are characterized by very similar CO_2 adsorption energy (compare the values in Table 1 and Table 2 for **1'**, **2'** and **16**, **17**, **18**). Complementary techniques besides microcalorimetry are necessary in order to identify the adsorption sites: in particular, insight on the nature of the involved sites can be obtained by considering the shift of the CO_2 modes and/or of the MOFs vibrations by means of infrared spectroscopy.

Table 2. Calculated dissociation energy, adsorption enthalpy [kJ mol^{-1}], and shifts of the CO_2 vibrational modes [cm^{-1}] with respect to the gas phase for the adducts reported in Figure 2 (MP2/TZVp level). All the energetic values are BSSE corrected. The sign of the CO_2 vibrational mode shifts upon interaction with isolated positive ($q > 0$) and negative ($q < 0$) point charges is also reported for comparison.

system	D_0^c	ΔH^c	$\Delta\tilde{\nu}_2$ [a]	$\Delta\tilde{\nu}_1$ [a]	$\Delta\tilde{\nu}_3$ [a]
$q > 0$[45]			>0	<0	>0
$q < 0$[47]			<0 and > 0	>0	<0
1	7.6	5.4	-2/-14	-1	-3
2a	11.6	9.7	-2/-16	1	-1
3	13.9	12.2	1/-17	1	0
4	9.2	7.4	4/-25	0	-2
5a	10.3	8.9	3/-22	0	-1
8	9.2	7.6	5/-28	0	-2
9	24.8	24.2	-7/-43	0	-1
11	9.5	7.2	-5/-11	-1	-3
12a	7.9	5.8	-5/-8	-1	-3
13a	8.3	5.8	-4/-13	-1	-4
14a	9.8	7.7	-4/-10	0	-2
15	7.4	5.6	4/-12	2	3
16	8.6	6.9	-1/12	3	5
17	7.3	5.3	-5/19	2	3
18	6.4	4.5	-1/-5	3	4

[a] Calculated vibrational modes for isolated CO_2 in the gas phase: $\tilde{\nu}_2$ = 640.9, $\tilde{\nu}_1$ = 1310.8 and $\tilde{\nu}_3$ = 2368.3 cm^{-1}.

In Table 2 the shift of the CO_2 vibrational modes is reported as calculated for a subset of the adducts under study. From a quick look at this table it is evident that very similar spectra are expected for different materials, independently on the adsorption energy. In fact, it was not possible to identify a simple relation between the CO_2 shifts and BE^c. The same conclusions can be drawn from the experimental data reviewed in Table 3: for example it is evident as the spectra obtained on UiO-66 isostructural MOFs are almost identical, independently on the functionality present on the linker. Coming back to the calculated data reported in Table 2, it is evident as whereas $\tilde{\nu}_1$ and $\tilde{\nu}_3$ are almost unperturbed by the adsorption, $\tilde{\nu}_2$ results to be split in two components where one remains close to the gas phase value ($|\Delta\tilde{\nu}_2| \leq 5$ cm^{-1}) whereas the other is redshifted of some tens of cm^{-1}. The larger sensitivity of $\tilde{\nu}_2$ with respect to the most common used $\tilde{\nu}_3$ has been observed experimentally for the interaction of CO_2 with polymers.[13] The greater sensitivity of $\tilde{\nu}_2$ has also been demonstrated in studies on the CO_2 solubility in liquids.[51] In such a kind of systems, the width of the ν_2 band can be also used to estimate the strength of interaction between CO_2 and polymers.[13] Unfortunately this region of the spectrum is complicated by the presence of the $^{13}CO_2$ bending modes that being only 20 cm^{-1} redshifted with respect to the $^{12}CO_2$ ones makes more difficult the determination of the shift (the vibration of the $^{13}CO_2$ in the gas phase can be superimposed to that corresponding to the adsorbed $^{12}CO_2$).

Table 3. Review of the CO_2 vibrational frequencies [cm^{-1}] as obtained experimentally for its adsorption on MOFs at room temperature in different pressure *P* conditions [mbar]. The frequencies for the two most abundant CO_2 isotopes in the gas phase and the frequencies reported for $^{12}CO_2$ after the adsorption in silicalite and polystyrene are also reported.

system	*P*	$\tilde{\nu}_2$	$\tilde{\nu}_1$	$\tilde{\nu}_3$
Gas ($^{12}CO_2$)[45]		667.3	1388.3	2349.3
Gas ($^{13}CO_2$)[52]		649	1334	2283
Silicalite[45, 53]	< 1	662		2341
PS[13]		657.2		2334.9
UiO-66[22]	0.72			2340
UiO-66-NH_2[22]	0.72			2337
UiO-66-NO_2[22, 54]	0.72	685, 669, 659, 649		2339
UiO-66-Br[22, 54]	0.72	684, 669, 662, 657, 649		2338
MIL-53(Cr)[55, 56]	11	669, 662, 650		2335
MIL-53(Al)[55]		661, 649		
MIL-53(Al)-NH_2[20]	200	669, 667, 661, 655, 649		2334
IRMOF-3[14, 20]		669, 667, 653		
HKUST-1				2333
CPO-27-Mg				2353
Ni-DBM-BPy[57]	2000	661, 645		2333

The results reported in Table 3 (experimental data) and in Table 2 (computational results) allow to make some relevant conclusions analyzing the $\Delta\tilde{\nu}_3$ values. In particular: (i) blueshift is due to interactions where the "oxygen component" is prevalent (as for the interaction with the N=N pair in **5** or with the hydroxyls); (ii) redshift is observed when the "carbon component" is playing the main role (as in the clusters representing the organic component of the material); (iii) an unperturbed $\tilde{\nu}_3$ is obtained when these two components are balancing each other (as for **3**). This observation is important as it can guide the localization of CO_2 in the materials and in visualize which is its coordination geometry.

Additional information can be obtained from the shift of the functional group modes. For what concerns the $-NH_2$ stretching

modes, the calculations indicate that if the amino group is directly interacting with CO_2 both its symmetric and asymmetric stretching modes would be redshifted of about –10 cm^{-1}: -10 and –10 cm^{-1} in **2**, -8 and –8 cm^{-1} in **4**, -9 and –8 cm^{-1} in **5** and -9 and –8 cm^{-1} in **8** (a negligible shift for the not interacting NH_2 is also predicted in **8**). Also in **3** the two asymmetric stretching frequencies are redshifted of –5 and –9 cm^{-1}, whereas for the symmetric modes a shift of –5 cm^{-1} was calculated. These shifts agree with those observed experimentally by Farbos et al.[42] for the symmetric stretching mode of $–NH_2$ in aromatic amine in supercritical CO_2 at 80 bar and 40°C: -9 cm^{-1} for aniline, -15 cm^{-1} for 1,4-benzene-diamine and of –7 cm^{-1} for 1,3-benzene-diamine. Shifts of the same order of magnitude are expected for the $–N_3$ (-7 cm^{-1}, **11**) and $–NO_2$ (-3/+3 cm^{-1}, **13**) groups.

If the sites involved directly in the interaction with CO_2 would be hydroxyl species, even larger shifts of their modes are expected: $\Delta\tilde{\nu}_{OH}$ of –12 (**15**), -44 (**16**), -30 (**17**), and –26 (**18**) cm^{-1} have been calculated. These values are of the same order of magnitude of the $\Delta\tilde{\nu}_{OH}$ reported in refs. [55, 56] for CO_2 adsorption in MIL-53(Cr) (-19 cm^{-1}).

In order to allow the comparison between the calculated CO_2 vibrational frequencies and those reported experimentally for MOFs, it is important to remind as in the case of the adsorption on microporous materials, it is not correct to take as reference for the unperturbed molecule the gas phase value for $\tilde{\nu}_3$ because of the large matrix effect due to the confinement.[45] For this reason, the $\tilde{\nu}_3$ value observed in silicalite, because of its apolar framework is in general taken as reference.[39, 45, 58] However, although lacking of cations, silicalite is not lacking of possible adsorption sites represented by silanols. By looking at the data reported in Table 2 it is evident that in spite of the weak interaction, a silanol would be able to shift upwards the $\tilde{\nu}_3$ mode of +3 cm^{-1}. On the basis of that, a reasonable value for the unperturbed CO_2 in a microporous matrix of 2338 cm^{-1} will be adopted in the following. This value is even in better agreement with that calculated for unperturbed CO_2 in Ref. [45]. A $\Delta\tilde{\nu}_3 > 0$ was reported for UiO-66 (+2 cm^{-1}), UiO-66-NO_2 (+1) and CPO-27-Mg (+15) as expected for the interaction with –OH (**15**-**18** clusters), -NO_2 (**12**) and open metal cations (**9**) respectively. Unexpectedly for MIL-53(Cr) a $\Delta\tilde{\nu}_3 < 0$ was observed in apparent contrast with the contemporaneous shift of the hydroxyls modes that would ask for a $\Delta\tilde{\nu}_3 > 0$. However, this contradiction is ascribable to the completely different arrangement of CO_2 in MIL-53 material in their narrow pore conformation (verified at lower CO_2 coverage): in fact, molecular mechanics and density functional calculations performed on a periodic model[34, 49] both indicate that in this case, because of the suitable distance between the two hydroxyls rows on the opposite sides of the pore, CO_2 would be able to interact contemporaneously with two -OH. Only at pressure higher than 6 bar, that is when the adsorption is carried out by the larger pore conformer a blue shit of the stretching mode would be observable.

Conclusions

Different functional groups have been tested for their affinity toward CO_2 by means of quantum-mechanical calculations. As a general remark it is observed that in the absence of strongly polarizing sites, the BEs are small and only slightly dependent on the adsorption system. BEs are all comprised in the interval between 8.8 (for the aromatic amine in 2-amino-terephatalate, **2'**) and 17.1 kJ mol^{-1} (for the aliphatic tertiary amine of 4-dimethylaminomethylene-1,2,3-triazole-1-phenyl, **6**). If on the contrary highly polarizing species are present, like open cations (e.g. Zn^{2+} or H^+), the affinity of these sites easily overcomes that of other sites. It is not accidental that the two largest BE belongs to 3-Zn-di-1,2,3-triazole (**9**) and adenine (**14**) where CO_2 is adsorbed on a Zn^{2+} and H^+ cation respectively. In general a side-on geometry of interaction for CO_2 is observed, independently on the predominant negative/positive values of the electrostatic potential on the cluster. On this basis it can be predicted that the CO_2 geometry of interaction with materials is the side-on one. This is opposite to what happens in the gas phase for the interaction with bare positive or negative charges. This hypothesis was confirmed on the basis of literature data that indicate that upon interaction the CO_2 bending mode is always followed by the spitting of the degenerate bending mode in two separate components.

For what concerns the amines, a large variety of species have been considered in this study, chosen between those already reported in literature and by proposing some new functionalities. The cluster calculations allowed to confirm the larger affinity towards CO_2 of aliphatic amines with respect to aromatic amines, as expected on the basis of their greater basicity. In particular, among the amino species studied the 4-dimethylaminomethylene-1,2,3-triazole-1-phenyl is predicted to be able to improve the MOF affinity toward CO_2 in separation/adsorption processes with respect to similar systems proposed in the literature up to now.

For what concerns the use of infrared spectroscopy as a method to characterize CO_2 adsorption in materials the calculations indicates as the stretching modes are quite insensitive to the adsorption energy, being shifted of only a few cm^{-1}. A larger difference between the signals can be obtained by looking at the CO_2 bending modes or, even better, to the shift of the functional groups involved in the interaction. It is also predicted in accordance with experiments[22] that the observation of IR vibrations is not able to discriminate between different adsorption functionalities present on the organic linker (same spectra for different materials). In the end, on the basis of the present calculations an attempt to assign the adsorption sites in different MOFs has been made on the basis of the experimental isosteric heats and spectroscopic signals.

The present calculations also indicate as $–NH_2$ pairs occasionally occurring in amino-terephatalate based MOFs, as the sites actually responsible for the improved performances of amino-terephtalate based MOFs, among the most studied material for CO_2 adsorption and separation.

Experimental Section

Computational methods. The calculations have been performed with the *Gaussian 09* software package.[59] All the systems under study have been optimized by means of the post-Hartree Fock perturbative Møller-Plesset method truncated at second-order (MP2) [60] in the frozen-core approximation. The use of MP2 was necessary because of the significant role of the dispersion forces in the interaction.[19, 33, 40] The inadequacy of less expensive DFT methods, was verified by applying the B3-LYP method to a subset of the complexes here studied. For the hydrogen atoms, the standard Pople basis set supplemented by diffuse and polarizability functions 6-31+G(d,p) has been adopted.[61] For In, an effective core potential (ECP) has been used to replace the innermost core electrons whereas the outermost core orbitals has been treated utilizing a double-ζ contraction[62] (Lanl2DZ). The C, N, O, Br, Si, Al and Ga elements have been modeled by means of the fully optimized triple-ζ valence basis sets proposed by Ahlrichs *et al.*[63] with polarization (TZVp). The C, N, O and Br basis set has been augmented by two sets of polarization functions derived from the original ones following

an even-tempered recipe that is by substituting the polarization orbital in the basis set with two orbitals, having respectively the coefficient doubled and halved with respect to the parent orbital. The so obtained basis sets will be indicated as TZV2p in the following. Geometry optimization has been carried out by means of the Berny optimization algorithm with analytical gradient. The thresholds were set to 0.000450 and 0.000300 a.u. for the maximum and the rms forces respectively; and to 0.001800 and 0.001200 a.u. for the maximum and rms atomic displacements, respectively. A (99,590) pruned grid was used (i.e. 99 radial points and 590 angular points per radial point). No symmetry constraints have been imposed.

Harmonic frequencies have been obtained by analytically determining the second derivatives of the energy with respect to the Cartesian nuclear coordinates and then transforming them to mass-weighted coordinates. No scaling factor has been adopted. The dissociation energy from the ground state (D_0) of the adducts was calculated from the corresponding dissociation energy from the potential energy minimum D_e by including the zero point energies (ZPE) of reactants and products. The ZPE was calculated in the harmonic approximation. The enthalpy variations (ΔH_{ads}) at standard conditions (298.15 K and 1 atm) were derived from the reaction energies including the ZPE and temperature corrections. The temperature corrections were computed using the standard expressions for an ideal gas in the canonical ensemble. No scaling factors were adopted. All the energetic data have been corrected for the basis set superposition error (BSSE) following the a posteriori method proposed by Boys and Bernardi[64] as implemented in *Gaussian 09*. The BSSE corrected energetic values are signalized by a c superscript and were obtained from the computed Y values as $Y^c = Y$ - BSSE.

Acknowledgements

Financial support by European VI framework through STREP project MOFCAT Contract number: NMP4-CT-2006-033335 and by European VII framework through STREP project NANOMOF Contract number: FP7-NMP-2008-LARGE-2 are gratefully acknowledged. Prof. Adriano Zecchina and Prof. David Farrusseng are acknowledged for fruitful discussions.

Keywords: Carbon dioxide fixation, Amines, Metal-organic frameworks, Density functional calculations, supercritical solvent.

Received: ((will be filled in by the editorial staff))
Published online: ((will be filled in by the editorial staff))

Entry for the Table of Contents

FULL PAPER

MOFs as CO_2 scrubbers. Quantum mechanics is used as screening tool to investigate the affinity toward CO_2 of different functional groups. The calculations explained the large CO_2 affinity observed experimentally for 2-amino-1,4-benzenedicarboxylate-based materials by the presence of pairs of $–NH_2$ groups and not by the direct interaction with isolated $–NH_2$ groups.

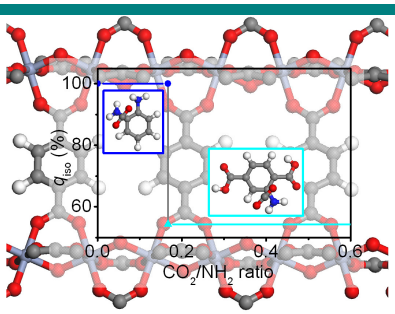

Jenny G. Vitillo, Marie Savonnet, Gabriele Ricchiardi and Silvia Bordiga*

Page No. – Page No.

Tailoring MOFs for CO_2 capture: the amino-effect

[1] EPICA, *Nature* **2004**, *429*, 623; J. R. Petit, et al., *Nature* **1999**, *399*, 429.
[2] C. D. Keeling, T. P. Whorf, Carbon Dioxide Research Group del Scripps Institution of Oceanography (SIO), *University of California, La Jolla, California USA 92093-0444*, (http://cdiac.esd.ornl.gov/ftp/maunaloa.
[3] D. W. Keith, M. Ha-Duong, J. K. Stolaroff, *Clim. Change* **2006**, *74*, 17; K. S. Lackner, *Sci.Am.* **2010**, *302*, 66; V. Nikulshina, A. Steinfeld, *Chem. Eng. J.* **2009**, *155*, 867; M. C. MacCracken, *Environ. Res. Lett.* **2009**, *4*; K. S. Lackner, *Eur. Phys. J.-Spec. Top.* **2009**, *176*, 93.
[4] D. M. D'Alessandro, B. Smit, J. R. Long, *Angew. Chem.-Int. Edit.* **2010**, *49*, 6058.
[5] S. R. Caskey, A. G. Wong-Foy, A. J. Matzger, *J. Am. Chem. Soc.* **2008**, *130*, 10870.
[6] A. L. Goodman, L. A. Campus, K. T. Schroeder, *Energy Fuels* **2005**, *19*, 471.
[7] J. C. Hicks, J. H. Drese, D. J. Fauth, M. L. Gray, G. G. Qi, C. W. Jones, *J. Am. Chem. Soc.* **2008**, *130*, 2902.
[8] M. Nainar, A. Veawab, *Ind. Eng. Chem. Res.* **2009**, *48*, 9299; A. Veawab, P. Tontiwachwuthikul, A. Chakma, *Ind. Eng. Chem. Res.* **1999**, *38*, 3917.
[9] R. Serna-Guerrero, E. Da'na, A. Sayari, *Ind. Eng. Chem. Res.* **2008**, *47*, 9406.
[10] R. Srivastava, D. Srinivas, P. Ratnasamy, *Appl. Catal. A* **2005**, *289*, 128.
[11] X. C. Xu, C. S. Song, J. M. Andresen, B. G. Miller, A. W. Scaroni, *Energy Fuels* **2002**, *16*, 1463; R. Srivastava, D. Srinivas, P. Ratnasamy, *J. Catal.* **2005**, *233*, 1; R. Srivastava, D. Srinivas, P. Ratnasamy, *Micropor. Mesopor. Mater.* **2006**, *90*, 314.
[12] A. Dibenedetto, C. Pastore, C. Fragale, M. Aresta, *ChemSusChem* **2008**, *1*, 742.
[13] S. G. Kazarian, M. F. Vincent, F. V. Bright, C. L. Liotta, C. A. Eckert, *J. Am. Chem. Soc.* **1996**, *118*, 1729.
[14] S. Couck, J. F. M. Denayer, G. V. Baron, T. Remy, J. Gascon, F. Kapteijn, **2009**, *131*, 6326.
[15] J. L. Song, Z. F. Zhang, S. Q. Hu, T. B. Wu, T. Jiang, B. X. Han, *Green Chem.* **2009**, *11*, 1031; R. Vaidhyanathan, S. S. Iremonger, K. W. Dawson, G. K. H. Shimizu, *Chem. Commun.* **2009**, 5230.
[16] A. Demessence, D. M. D'Alessandro, M. L. Foo, J. R. Long, *J. Am. Chem. Soc.* **2009**, *131*, 8784.
[17] Y. K. Hwang, et al., *Angew. Chem.-Int. Edit.* **2008**, *47*, 4144.
[18] A. Phan, C. J. Doonan, F. J. Uribe-Romo, C. B. Knobler, M. O'Keeffe, O. M. Yaghi, *Acc. Chem. Res.* **2009**, *43*, 58.
[19] B. Arstad, H. Fjellvag, K. O. Kongshaug, O. Swang, R. Blom, *Adsorption* **2008**, *14*, 755.
[20] J. Gascon, U. Aktay, M. D. Hernandez-Alonso, G. P. M. van Klink, F. Kapteijn, *J. Catal.* **2009**, *261*, 75.
[21] S. Bauer, C. Serre, T. Devic, P. Horcajada, J. Marrot, G. Ferey, N. Stock, *Inorg. Chem.* **2008**, *47*, 7568.

[22] M. Kandiah, et al., **2010**, accepted.
[23] P. J. E. Harlick, A. Sayari, *Ind. Eng. Chem. Res.* **2006**, *45*, 3248.
[24] M. J. Ingleson, J. P. Barrio, J. B. Guilbaud, Y. Z. Khimyak, M. J. Rosseinsky, *Chem. Commun.* **2008**, 2680; O. M. Yaghi, M. O'Keeffe, N. W. Ockwig, H. K. Chae, M. Eddaoudi, J. Kim, *Nature* **2003**, *423*, 705; M. Eddaoudi, J. Kim, N. Rosi, D. Vodak, J. Wachter, M. O'Keeffe, O. M. Yaghi, *Science* **2002**, *295*, 469.
[25] J. L. C. Rowsell, O. M. Yaghi, *J. Am. Chem. Soc.* **2006**, *128*, 1304.
[26] A. R. Millward, O. M. Yaghi, *J. Am. Chem. Soc.* **2005**, *127*, 17998.
[27] P. L. Llewellyn, S. Bourrelly, C. Serre, Y. Filinchuk, G. Férey, **2006**, *45*, 7751.
[28] E. Neofotistou, C. D. Malliakas, P. N. Trikalitis, *Chem.-Eur. J.* **2009**, *15*, 4523.
[29] A. Comotti, S. Bracco, P. Sozzani, S. Horike, R. Matsuda, J. Chen, M. Takata, Y. Kubota, S. Kitagawa, *J. Am. Chem. Soc.* **2008**, *130*, 13664.
[30] H. Kim, Y. Kim, M. Yoon, S. Linn, S. M. Park, G. Seo, K. Kim, *J. Am. Chem. Soc.* **2010**, *132*, 12200.
[31] M. Xue, Y. Liu, R. M. Schaffino, S. C. Xiang, X. J. Zhao, G. S. Zhu, S. L. Qiu, B. L. Chen, *Inorg. Chem.* **2009**, *48*, 4649; M. Tagliabue, D. Farrusseng, S. Valencia, S. Aguado, U. Ravon, C. Rizzo, A. Corma, C. Mirodatos, *Chem. Eng. J.* **2009**, *155*, 553.
[32] H. Hayashi, A. P. Cote, H. Furukawa, M. O'Keeffe, O. M. Yaghi, *Nat. Mater.* **2007**, *6*, 501.
[33] K. D. Vogiatzis, A. Mavrandonakis, W. Klopper, G. E. Froudakis, *ChemPhysChem* **2009**, *10*, 374.
[34] E. Stavitski, E. A. Pidko, S. Couck, T. Remy, E. J. M. Hensen, B. M. Weckhuysen, J. Denayer, J. Gascon, F. Kapteijn, *Langmuir* **2011**, *27*, 3970.
[35] O. M. Yaghi, *FY 2009 Annual Progress Report, DOE Hydrogen Program* **2009**.
[36] M. Savonnet, D. Bazer-Bachi, N. Bats, J. Perez-Pellitero, E. Jeanneau, V. Lecocq, C. Pinel, D. Farrusseng, *J. Am. Chem. Soc.* **2010**, *132*, 4518.
[37] A. Torrisi, C. Mellot-Draznieks, R. G. Bell, *J. Chem. Phys.* **2009**, *130*.
[38] A. Torrisi, C. Mellot-Draznieks, R. G. Bell, *J. Chem. Phys.* **2010**, *132*, 044705.
[39] L. Valenzano, B. Civalleri, S. Chavan, G. Turnes Palomino, C. Otero Areán, S. Bordiga, **2010**, *114*, 11185.
[40] B. Arstad, R. Blom, O. Swang, *J. Phys. Chem. A* **2007**, *111*, 1222.
[41] C. A. Eckert, B. L. Knutson, P. G. Debenedetti, *Nature* **1996**, *383*, 313; J. F. Brennecke, *Nature* **1997**, *389*, 333; O. S. Fleming, S. G. Kazarian, *Polymer Processing with Supercritical Fluids*, 205, Wiley-VCH Verlag GmbH & Co. KGaA, **2006**.
[42] B. Farbos, T. Tassaing, *Phys. Chem. Chem. Phys.* **2009**, *11*, 5052.
[43] B. Renault, E. Cloutet, H. Cramail, T. Tassaing, M. Besnard, *J. Phys. Chem. A* **2007**, *111*, 4181.
[44] C. Volkringer, et al., **2008**, *47*, 11892.
[45] B. Bonelli, B. Civalleri, B. Fubini, P. Ugliengo, C. Otero Areán, E. Garrone, **2000**, *104*, 10978.
[46] P. Raveendran, Y. Ikushima, S. L. Wallen, *Accounts Chem. Res.* **2005**, *38*, 478.
[47] J. M. Weber, H. Schneider, *J. Chem. Phys.* **2004**, *120*, 10056.
[48] R. Vaidhyanathan, S. S. Iremonger, G. K. H. Shimizu, P. G. Boyd, S. Alavi, T. K. Woo, *Science* **2010**, *330*, 650.
[49] N. A. Ramsahye, G. Maurin, S. Bourrelly, P. L. Llewellyn, T. Devic, C. Serre, T. Loiseau, G. Ferey, **2007**, *13*, 461.
[50] A. D. Hunter, V. Mozol, S. D. Tsai, *Organometallics* **1992**, *11*, 2251; J. G. Vitillo, E. Groppo, S. Bordiga, S. Chavan, G. Ricchiardi, A. Zecchina, *Inorg. Chem.* **2009**, *48*, 5439.
[51] C. Heald, *Proc. R. Soc.* **1962**, *A268*, 89; J. C. Dobrowolski, M. H. Jamroz, *J. Mol. Struct.* **1992**, *275*, 211.
[52] T. Shimanouchi, *Tables of Molecular Vibrational Frequencies Consolidated Vol. I*, 1, National Bureau of Standards, **1972**.
[53] S. K. Wirawan, D. Creaser, *Micro. Meso. Mat.* **2006**, *91*, 196.
[54] F. Bonino, private communication.
[55] A. Vimont, A. Travert, P. Bazin, J. C. Lavalley, M. Daturi, C. Serre, G. Ferey, S. Bourrelly, P. L. Llewellyn, *Chem. Commun.* **2007**, 3291.

[56] S. Bourrelly, P. L. Llewellyn, C. Serre, F. Millange, T. Loiseau, G. Ferey, **2005**, *127*, 13519.
[57] J. T. Culp, A. L. Goodman, D. Chirdon, S. G. Sankar, C. Matranga, *J. Phys. Chem. C* **2010**, *114*, 2184.
[58] M. Armandi, E. Garrone, C. Otero Arean, B. Bonelli, **2009**, *10*, 3316.
[59] M. J. Frisch, et al., Revision B.05 ed., Gaussian, Inc., Wallingford CT, **2004**.
[60] C. Møller, M. S. Plesset, **1934**, *46*, 618.
[61] T. Clark, J. Chandrasekhar, G. W. Spitznagel, P. v. R. Schleyer, *J. Comp. Chem.* **1983**, *4*, 294; M. J. Frisch, J. A. Pople, J. S. Binkley, *J. Chem. Phys.* **1984**, *80*, 3265.
[62] W. R. Wadt, P. J. Hay, **1985**, *82*, 284; P. J. Hay, W. R. Wadt, **1985**, *82*, 270.
[63] A. Schäfer, C. Huber, R. Ahlrichs, *J. Chem. Phys.* **1994**, *100*, 5829.
[64] S. F. Boys, F. Bernardi, *Mol. Phys.* **1970**, *19*, 553.